
MASS: MoErging through Adaptive Subspace Selection

Donato Crisostomi* Alessandro Zirilli*

Antonio Andrea Gargiulo Maria Sofia Bucarelli Simone Scardapane

Fabrizio Silvestri Iacopo Masi Emanuele Rodolà

Sapienza University of Rome

{crisostomi, zirilli, gargiulo, masi, rodola}@di.uniroma1.it
simone.scardapane@uniroma1.it {bucarelli, fsilvestri}@diag.uniroma1.it

Abstract

Model merging has emerged as a lightweight alternative to ensembling, combining multiple fine-tuned models into a single set of parameters without additional training. However, existing methods rarely match the accuracy of individually fine-tuned models. We introduce MASS (MoErging through Adaptive Subspace Selection), a training-free approach that narrows this gap while maintaining near state-of-the-art performance across tasks. MASS leverages low-rank decompositions of task-specific updates, storing only the most salient singular components and merging them into a shared model. At inference, a data-free, non-parametric router selects the most relevant subspace (or combination of subspaces) based on intermediate features. This adds only a two-pass inference overhead and a $\sim 2\times$ storage cost relative to a single pretrained model, regardless of the number of tasks. Evaluated on CLIP-based image classification with ViT-B-16, ViT-B-32, and ViT-L-14 across 8, 14, and 20 tasks, MASS achieves up to $\sim 98\%$ of the accuracy of separate fine-tuned models, establishing a new state-of-the-art while remaining far more storage-efficient than ensembling.

1 Introduction

Early deep learning models were trained from scratch, but the rise of large pretrained backbones shifted the focus to fine-tuning for specific tasks Devlin et al. [2019], Tan et al. [2018], Yosinski et al. [2014], Hu et al. [2022], Radford et al. [2021]. Today, the abundance of publicly available fine-tuned models¹ has sparked interest in *no-tuning* methods that exploit both the foundation model and existing fine-tuned endpoints.

Among these, *model merging* [Ilharco et al., 2023, Akiba et al., 2025, Yadav et al., 2023, Yu et al., 2024, Ainsworth et al., 2023, Crisostomi et al., 2025, Singh and Jaggi, 2020, Gargiulo et al., 2025, Zhou et al., 2024, Daheim et al.] offers a lightweight, storage-efficient alternative to ensembling by combining multiple fine-tuned models into a single parameter set. Early approaches such as **Task Arithmetic** [Ilharco et al., 2023] simply summed task vectors (fine-tuned minus pretrained weights), while later methods [Gargiulo et al., 2025, Daniel et al., 2025] preserved layer-wise structure for better accuracy. In particular, **Task Singular Vectors (TSV)** [Gargiulo et al., 2025] leveraged the low-rank structure of task updates, retaining most fine-tuned performance with only a few singular vectors per task.

However, current structured merging methods remain static: their aggregation weights do not adapt to the input, leading to suboptimal performance and significant accuracy drops for certain tasks.

¹<https://huggingface.co/docs/hub/models-the-hub>

To address this, we introduce **MASS** (*Mo-Erging through Adaptive Subspace Selection*), which integrates the adaptivity of Mixture-of-Experts (MoE) [Shazeer et al., 2017, Eigen et al., 2014, Fedus et al., 2022, Du et al., 2022] with singular-vector-based merging. MASS dynamically routes inputs to the most relevant task subspaces (Fig. 1) without requiring task data or additional tuning. This is a key advantage in scenarios where only model checkpoints are available.

We evaluate MASS on ViT-B-32, ViT-B-16, and ViT-L-14 backbones across 8, 14, and 20 tasks. Our method consistently outperforms existing merging techniques, recovering up to 95%–98% of the accuracy of individually fine-tuned models with only a modest overhead ($\sim 2\times$ inference and storage relative to the base model). In batched settings, MASS reduces accuracy loss to below 1% on most benchmarks.

Our key contributions are:

- Introducing MASS, a singular-vector-based merging method with adaptive input routing.
- Proposing a projection-based, data-free router that requires no additional fine-tuning.
- New state-of-the-art results in multitask merging across models and tasks.

2 Background

In this section, we introduce the key concepts underlying our approach.

Task Vectors Task Arithmetic (TA) [Ilharco et al., 2023] represents each task as a *task vector*, i.e., the difference between fine-tuned and pretrained weights. A multitask model for T tasks is obtained by summing these vectors:

$$\theta_{\text{MT}} = \theta_{\text{pre}} + \alpha \sum_{i=1}^T \tau_i, \quad (1)$$

where θ_{pre} are the pretrained weights, α is a scaling factor, and $\tau_i = \theta_{\text{ft}_i} - \theta_{\text{pre}}$ is the task vector for task i . Following Gargiulo et al. [2025], we consider this operation layer-wise:

$$\theta_{\text{MT}}^{(\ell)} = \theta_{\text{pre}}^{(\ell)} + \alpha \sum_{i=1}^T \Delta_i^{(\ell)}, \quad (2)$$

where $\Delta_i^{(\ell)} = \theta_{\text{ft}_i}^{(\ell)} - \theta_{\text{pre}}^{(\ell)}$ is the task-specific weight difference for layer ℓ . For matrix-shaped layers, $\Delta_i^{(\ell)}$ is referred to as the *per-layer task matrix*. For brevity, we omit the layer index.

Task Singular Vectors Gargiulo et al. [2025] show that task matrices Δ_i exhibit strong low-rank structure. For each task i , they compute the SVD:

$$\Delta_i = U_i \Sigma_i V_i^\top,$$

and truncate it to rank k , keeping the top- k singular vectors and values: \tilde{U}_i , \tilde{V}_i , and $\tilde{\Sigma}_i$. Stacking these across tasks yields $U = [\tilde{U}_1 \dots \tilde{U}_T]$ (left TSVs), $V = [\tilde{V}_1 \dots \tilde{V}_T]$ (right TSVs), and $\tilde{\Sigma}$ (block-diagonal with $\tilde{\Sigma}_i$). The multitask update is then expressed as:

$$\hat{\Delta} = U_\perp \Sigma V_\perp^\top, \quad (3)$$

where U_\perp and V_\perp^\top are orthogonalized to reduce inter-task interference. This effectively sums the top- k rank-one updates per task while ensuring the task subspaces remain distinct (see Alg. 1 in the Appendix).

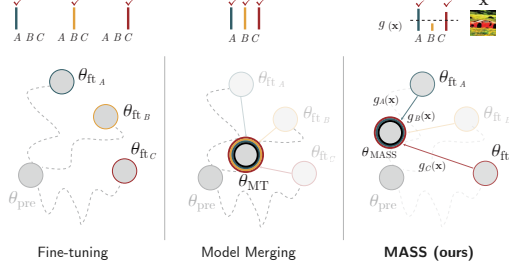


Figure 1: (left) Fine-tuning creates separate models for tasks A, B, and C. (middle) Model merging combines their task vectors {A, B, C} using a fixed aggregation. (right) MASS stores θ_{pre} and orthogonalized task singular vectors V_\perp^\top , and adaptively merges them at test time via a routing function $g(\mathbf{x})$ that selects task subspaces based on input features.

| | Method | ViT-B-32 | | | ViT-B-16 | | | ViT-L-14 | | |
|-------|---------------------------------------|------------------------|------------------------|------------------------|------------------------|------------------------|------------------------|------------------------|------------------------|------------------------|
| | | 8 tasks | 14 tasks | 20 tasks | 8 tasks | 14 tasks | 20 tasks | 8 tasks | 14 tasks | 20 tasks |
| Base | Zeroshot | 48.2 _(53.5) | 57.2 _(63.6) | 56.1 _(62.4) | 55.3 _(59.3) | 61.2 _(66.1) | 59.7 _(64.5) | 64.7 _(68.0) | 68.2 _(72.1) | 65.2 _(68.9) |
| | Finetuned | 92.8 _(1.00) | 90.8 _(1.00) | 91.3 _(1.00) | 94.6 _(1.00) | 92.7 _(1.00) | 93.1 _(1.00) | 95.8 _(1.00) | 94.2 _(1.00) | 94.7 _(1.00) |
| | Weight Averaging | 66.3 _(72.1) | 64.3 _(71.1) | 61.0 _(67.5) | 72.2 _(76.6) | 69.4 _(74.8) | 65.3 _(70.3) | 79.5 _(83.1) | 76.7 _(81.1) | 71.6 _(75.6) |
| Fixed | Task Arithmetic Ilharco et al. [2023] | 70.7 _(76.5) | 65.3 _(72.0) | 60.5 _(66.7) | 75.4 _(79.5) | 70.5 _(75.8) | 65.7 _(70.7) | 84.9 _(88.6) | 79.4 _(83.9) | 74.0 _(78.0) |
| | Consensus TA Wang et al. [2024] | 75.0 _(80.8) | 70.3 _(77.3) | 65.4 _(71.9) | 79.3 _(83.8) | 74.3 _(79.9) | 69.7 _(74.9) | 86.3 _(90.0) | 82.2 _(86.9) | 79.0 _(83.2) |
| | TSV-M Gargiulo et al. [2025] | 85.8 _(92.3) | 80.0 _(87.8) | 77.0 _(84.2) | 89.0 _(93.9) | 84.5 _(91.0) | 80.5 _(86.4) | 92.9 _(96.9) | 89.1 _(94.4) | 87.7 _(92.5) |
| | Iso-C Daniel et al. [2025] | 86.3 _(92.9) | 80.3 _(88.1) | 75.5 _(82.5) | 90.6 _(95.6) | 84.8 _(91.1) | 79.6 _(85.4) | 94.2 _(98.3) | 89.3 _(94.5) | 87.6 _(92.2) |
| | Iso-CTS Daniel et al. [2025] | 86.2 _(92.8) | 81.7 _(89.7) | 78.1 _(85.5) | 91.1 _(96.1) | 86.4 _(92.8) | 82.4 _(88.4) | 94.7 _(98.8) | 91.0 _(96.3) | 90.1 _(94.9) |
| MoE | MASS | 90.6 _(97.6) | 86.8 _(95.5) | 84.4 _(92.5) | 93.2 _(98.5) | 90.2 _(97.3) | 85.3 _(91.9) | 94.6 _(98.7) | 91.4 _(97.0) | 90.6 _(95.7) |

Table 1: Average absolute accuracy results on model merging benchmarks; subscript (in parentheses) is the normalized average accuracy.

3 Approach

Our approach consists of a one-time *fixed merging* step and an *adaptive inference* step.

Fixed merging. We first merge task-specific updates using TSV-M Gargiulo et al. [2025] to produce an encoder θ_{MT} capable of separating task subspaces. This step is input-independent and performed only once.

Adaptive inference. At test time, MASS dynamically routes each input \mathbf{x} through four steps:

- (i) **First pass:** forward \mathbf{x} through θ_{MT} ;
- (ii) **Routing:** compute the projection residual of intermediate activations onto each task subspace and select the lowest-residual tasks;
- (iii) **Adaptive merge:** combine the selected subspaces into Δ_{ada} ;
- (iv) **Second pass:** predict with $\theta_{\text{pre}} + \alpha\Delta_{\text{ada}}$.

Projection-based routing. Unlike existing routers, which require task data or additional training, our router is entirely data-free. For activations \mathbf{z}_ℓ at a chosen layer, we compute:

$$r_i = \|\mathbf{z}_\ell - V_i V_i^\top \mathbf{z}_\ell\|_2, \quad (4)$$

where V_i is the matrix of right singular vectors for task i . Tasks with residuals below a threshold η are selected. To prevent redundant directions from dominating, we discard highly similar subspaces during fixed merging using a cosine-similarity filter.

Adaptive merging and prediction. The selected subspaces Ω are merged via TSV-M to obtain θ_{MASS} . Each corresponding task head h_i produces logits \mathbf{z}_i , and the head with the highest confidence determines the final prediction:

$$(i^*, c^*) = \arg \max_{(i, c) \in \Omega \times \{1, \dots, C_i\}} z_i[c].$$

This enables MASS to operate without prior knowledge of the task, adapting its merging and classification on a per-input basis.

4 Experiments

Models and baselines We run experiments on three CLIP Radford et al. [2021] variants with ViT Dosovitskiy et al. [2021] encoders: ViT-B-32, ViT-B-16, and ViT-L-14. Baselines include training-free methods such as weight averaging, Task Arithmetic Ilharco et al. [2023], and Consensus Merging Wang et al. [2024]. Zero-shot accuracy provides a null reference, while the mean accuracy of individually fine-tuned models serves as the upper bound. We refer to the Appendix for details on our benchmark.

MoErging results Tab. 1 shows that MASS sets a new state of the art across all model sizes and task counts, outperforming both classic methods (Task Arithmetic [Ilharco et al., 2023], Consensus TA [Wang et al., 2024]) and newer ones (Iso-C, Iso-CTS [Daniel et al., 2025]).

On the 20-task benchmark, MASS improves absolute accuracy over the fixed TSV-M baseline by +7.4% (ViT-B-32), +4.8% (ViT-B-16), and +2.9% (ViT-L-14), while retaining a higher fraction of each model’s fine-tuned performance. Gains are largest on smaller backbones, suggesting that routing more effectively mitigates task interference when capacity is limited.

Per-task results (Fig. 2) show consistent improvements, with accuracy retention above 80% for nearly all tasks (even in the 20-task setting) and above 94% in the 8-task benchmark.

Under the 8-task benchmark on ViT-B-32, MASS reaches 97.6% normalized accuracy, surpassing TwinMerging’s 95.3% despite not assuming oracle knowledge of the correct head.

Choosing a routing layer We analyze the impact of routing layer choice on task accuracy (Fig. 3 in the Appendix). Both ViT-B-32 and ViT-B-16 achieve peak performance at layer 9, with MLP layers slightly outperforming attention layers.

Accuracy, however, varies widely by task, with standard deviations up to 40% across layers. As shown in Fig. 3c, STL10 benefits from earlier layers ($\ell = 3-5$), while SUN397 performs best at later ones ($\ell = 9-11$). This suggests that optimal routing layers are task-dependent, motivating future work on adaptive selection.

| MASS | ViT-B-32 | | | ViT-B-16 | | |
|-----------------------|-------------|-------------|-------------|-------------|-------------|-------------|
| | + | 8 tasks | 14 tasks | 20 tasks | 8 tasks | 14 tasks |
| nn | 94.5 | 91.3 | 91.3 | 93.5 | 91.7 | 86.5 |
| mlp | 98.9 | 98.2 | 96.4 | 98.9 | 98.4 | 95.0 |
| proj _{PRE} | 96.2 | 90.4 | 76.7 | 97.9 | 97.3 | 81.1 |
| proj _{TSV-M} | 97.6 | 95.5 | 92.5 | 98.5 | 97.3 | 91.9 |

Table 2: Average normalized accuracy for different routers.

MLP f_θ on validation embeddings to predict task identity; while accurate, this approach relies on labeled task data, which is often unavailable in practical merging scenarios.

Tab. 2 shows that NN performs well but slightly below MASS, while the MLP achieves the highest accuracy but with limited applicability due to its data requirement. Our projection-based router (proj) offers the best balance: starting from TSV-M (proj_{TSV-M}) outperforms routing from the pretrained backbone (proj_{PRE}), as the orthogonal subspaces created by TSV-M make residual-based selection effective without any labels or additional training.

5 Conclusions

In this paper, we introduced MASS, a merging approach that leverages low-rank task updates while adaptively routing each input to the most relevant subspace. To address the lack of per-task datasets in real-world scenarios, MASS uses a fully data- and training-free projection-based router.

Experiments show that MASS achieves state-of-the-art results, recovering nearly the full accuracy of individual task-specific models at a fraction of their combined storage cost. Future work includes refining the router for finer subspace selection and extending MASS to out-of-distribution scenarios, where task subspaces could be combined on the fly to tackle unseen tasks.

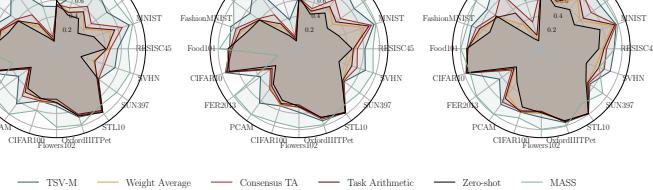


Figure 2: Normalized task accuracies for ViT-B-32, ViT-B-16, and ViT-L-14 on the 20-task benchmark.

Comparison with other routers Finally, we compare MASS with two common routing strategies, namely:

(i) **Nearest Neighbor (NN)**, which builds a small support set from each task’s validation data and assigns a test sample to the nearest embedding; this requires no extra parameters but assumes access to and storage of validation data.

(ii) **MLP router**, which trains an MLP f_θ on validation embeddings to predict task identity; while accurate, this approach relies on labeled task data, which is often unavailable in practical merging scenarios.

References

Samuel K. Ainsworth, Jonathan Hayase, and Siddhartha S. Srinivasa. Git re-basin: Merging models modulo permutation symmetries. In *The Eleventh International Conference on Learning Representations, ICLR 2023, Kigali, Rwanda, May 1-5, 2023*, 2023.

Takuya Akiba, Makoto Shing, Yujin Tang, Qi Sun, and David Ha. Evolutionary optimization of model merging recipes. *Nature Machine Intelligence*, 2025. ISSN 2522-5839.

Lukas Bossard, Matthieu Guillaumin, and Luc Van Gool. Food-101 – Mining Discriminative Components with Random Forests. In David Fleet, Tomas Pajdla, Bernt Schiele, and Tinne Tuytelaars, editors, *Computer Vision – ECCV 2014*, pages 446–461, Cham, 2014. Springer International Publishing. ISBN 978-3-319-10599-4. doi: 10.1007/978-3-319-10599-4_29.

Gong Cheng, Junwei Han, and Xiaoqiang Lu. Remote Sensing Image Scene Classification: Benchmark and State of the Art. *Proceedings of the IEEE*, 105(10):1865–1883, October 2017. ISSN 1558-2256. doi: 10.1109/JPROC.2017.2675998. Conference Name: Proceedings of the IEEE.

Mircea Cimpoi, Subhransu Maji, Iasonas Kokkinos, Sammy Mohamed, and Andrea Vedaldi. Describing Textures in the Wild. In *2014 IEEE Conference on Computer Vision and Pattern Recognition*, pages 3606–3613, Columbus, OH, USA, June 2014. IEEE. ISBN 978-1-4799-5118-5. doi: 10.1109/CVPR.2014.461.

Tarin Clanuwat, Mikel Bober-Irizar, Asanobu Kitamoto, Alex Lamb, Kazuaki Yamamoto, and David Ha. Deep Learning for Classical Japanese Literature, November 2018. URL <http://arxiv.org/abs/1812.01718>. arXiv:1812.01718 [cs, stat].

Adam Coates, Andrew Ng, and Honglak Lee. An Analysis of Single-Layer Networks in Unsupervised Feature Learning. In *Proceedings of the Fourteenth International Conference on Artificial Intelligence and Statistics*, pages 215–223. JMLR Workshop and Conference Proceedings, June 2011. URL <https://proceedings.mlr.press/v15/coates11a.html>. ISSN: 1938-7228.

Gregory Cohen, Saeed Afshar, Jonathan Tapson, and André van Schaik. EMNIST: Extending MNIST to handwritten letters. In *2017 International Joint Conference on Neural Networks (IJCNN)*, pages 2921–2926, May 2017. doi: 10.1109/IJCNN.2017.7966217. ISSN: 2161-4407.

Donato Crisostomi, Marco Fumero, Daniele Baieri, Florian Bernard, and Emanuele Rodolà. C^2M^3 : Cycle-consistent multi-model merging. In *Advances in Neural Information Processing Systems*, volume 37, 2025.

Nico Daheim, Thomas Möllenhoff, Edoardo Ponti, Iryna Gurevych, and Mohammad Emtiyaz Khan. Model merging by uncertainty-based gradient matching. In *The Twelfth International Conference on Learning Representations*.

Marczak Daniel, Magistri Simone, Cygert Sebastian, Twardowski Bartłomiej, D Bagdanov Andrew, and Joost van de Weijer. No task left behind: Isotropic model merging with common and task-specific subspaces. *ArXiv preprint*, 2025.

Jacob Devlin, Ming-Wei Chang, Kenton Lee, and Kristina Toutanova. Bert: Pre-training of deep bidirectional transformers for language understanding. In *Proceedings of the 2019 conference of the North American chapter of the association for computational linguistics: human language technologies, volume 1 (long and short papers)*, pages 4171–4186, 2019.

Alexey Dosovitskiy, Lucas Beyer, Alexander Kolesnikov, Dirk Weissenborn, Xiaohua Zhai, Thomas Unterthiner, Mostafa Dehghani, Matthias Minderer, Georg Heigold, Sylvain Gelly, Jakob Uszkoreit, and Neil Houlsby. An image is worth 16x16 words: Transformers for image recognition at scale, 2021. URL <https://arxiv.org/abs/2010.11929>.

Nan Du, Yanping Huang, Andrew M Dai, Simon Tong, Dmitry Lepikhin, Yuanzhong Xu, Maxim Krikun, Yanqi Zhou, Adams Wei Yu, Orhan Firat, et al. Glam: Efficient scaling of language models with mixture-of-experts. In *International conference on machine learning*, pages 5547–5569. PMLR, 2022.

David Eigen, Marc’Aurelio Ranzato, and Ilya Sutskever. Learning factored representations in a deep mixture of experts, 2014. URL <https://arxiv.org/abs/1312.4314>.

William Fedus, Barret Zoph, and Noam Shazeer. Switch transformers: Scaling to trillion parameter models with simple and efficient sparsity. *Journal of Machine Learning Research*, 23(120):1–39, 2022.

Antonio Andrea Gargiulo, Donato Crisostomi, Maria Sofia Bucarelli, Simone Scardapane, Fabrizio Silvestri, and Emanuele Rodolà. Task singular vectors: Reducing task interference in model merging. In *Proc. CVPR*, 2025.

Ian J. Goodfellow, Dumitru Erhan, Pierre Luc Carrier, Aaron Courville, Mehdi Mirza, Ben Hamner, Will Cukierski, Yichuan Tang, David Thaler, Dong-Hyun Lee, Yingbo Zhou, Chetan Ramaiah, Fangxiang Feng, Ruifan Li, Xiaojie Wang, Dimitris Athanasakis, John Shawe-Taylor, Maxim Milakov, John Park, Radu Ionescu, Marius Popescu, Cristian Grozea, James Bergstra, Jingjing Xie, Lukasz Romaszko, Bing Xu, Zhang Chuang, and Yoshua Bengio. Challenges in Representation Learning: A Report on Three Machine Learning Contests. In Minho Lee, Akira Hirose, Zeng-Guang Hou, and Rhee Man Kil, editors, *Neural Information Processing*, pages 117–124, Berlin, Heidelberg, 2013. Springer. ISBN 978-3-642-42051-1. doi: 10.1007/978-3-642-42051-1_16.

Patrick Helber, Benjamin Bischke, Andreas Dengel, and Damian Borth. EuroSAT: A Novel Dataset and Deep Learning Benchmark for Land Use and Land Cover Classification. *IEEE Journal of Selected Topics in Applied Earth Observations and Remote Sensing*, 12(7):2217–2226, July 2019. ISSN 2151-1535. doi: 10.1109/JSTARS.2019.2918242. Conference Name: IEEE Journal of Selected Topics in Applied Earth Observations and Remote Sensing.

Edward J Hu, Yelong Shen, Phillip Wallis, Zeyuan Allen-Zhu, Yuanzhi Li, Shean Wang, Lu Wang, Weizhu Chen, et al. Lora: Low-rank adaptation of large language models. *ICLR*, 1(2):3, 2022.

Gabriel Ilharco, Marco Túlio Ribeiro, Mitchell Wortsman, Ludwig Schmidt, Hannaneh Hajishirzi, and Ali Farhadi. Editing models with task arithmetic. In *The Eleventh International Conference on Learning Representations, ICLR 2023, Kigali, Rwanda, May 1-5, 2023*, 2023.

Jonathan Krause, Michael Stark, Jia Deng, and Li Fei-Fei. 3D Object Representations for Fine-Grained Categorization. In *2013 IEEE International Conference on Computer Vision Workshops*, pages 554–561, Sydney, Australia, December 2013. IEEE. ISBN 978-1-4799-3022-7. doi: 10.1109/ICCVW.2013.77.

Alex Krizhevsky and Geoffrey Hinton. Learning multiple layers of features from tiny images. Technical Report 0, University of Toronto, Toronto, Ontario, 2009. URL <https://www.cs.toronto.edu/~kriz/learning-features-2009-TR.pdf>.

Y. Lecun, L. Bottou, Y. Bengio, and P. Haffner. Gradient-based learning applied to document recognition. *Proceedings of the IEEE*, 86(11):2278–2324, 1998. doi: 10.1109/5.726791.

Yuval Netzer, Tao Wang, Adam Coates, Alessandro Bissacco, Bo Wu, and Andrew Y. Ng. Reading digits in natural images with unsupervised feature learning. In *NIPS Workshop on Deep Learning and Unsupervised Feature Learning 2011*, 2011. URL http://ufldl.stanford.edu/housenumbers/nips2011_housenumbers.pdf.

Maria-Elena Nilsback and Andrew Zisserman. Automated Flower Classification over a Large Number of Classes. In *2008 Sixth Indian Conference on Computer Vision, Graphics & Image Processing*, pages 722–729, December 2008. doi: 10.1109/ICVGIP.2008.47.

Omkar M Parkhi, Andrea Vedaldi, Andrew Zisserman, and C. V. Jawahar. Cats and dogs. In *2012 IEEE Conference on Computer Vision and Pattern Recognition*, pages 3498–3505, June 2012. doi: 10.1109/CVPR.2012.6248092. ISSN: 1063-6919.

Alec Radford, Jong Wook Kim, Chris Hallacy, Aditya Ramesh, Gabriel Goh, Sandhini Agarwal, Girish Sastry, Amanda Askell, Pamela Mishkin, Jack Clark, et al. Learning transferable visual models from natural language supervision. In *International conference on machine learning*, pages 8748–8763. PMLR, 2021.

Noam Shazeer, Azalia Mirhoseini, Krzysztof Maziarz, Andy Davis, Quoc Le, Geoffrey Hinton, and Jeff Dean. Outrageously large neural networks: The sparsely-gated mixture-of-experts layer, 2017. URL <https://arxiv.org/abs/1701.06538>.

Sidak Pal Singh and Martin Jaggi. Model fusion via optimal transport. In *Advances in Neural Information Processing Systems 33: Annual Conference on Neural Information Processing Systems 2020, NeurIPS 2020, December 6-12, 2020, virtual*, 2020.

Richard Socher, Alex Perelygin, Jean Wu, Jason Chuang, Christopher D. Manning, Andrew Ng, and Christopher Potts. Recursive deep models for semantic compositionality over a sentiment treebank. In David Yarowsky, Timothy Baldwin, Anna Korhonen, Karen Livescu, and Steven Bethard, editors, *Proceedings of the 2013 Conference on Empirical Methods in Natural Language Processing*, pages 1631–1642, Seattle, Washington, USA, October 2013. Association for Computational Linguistics. URL <https://aclanthology.org/D13-1170>.

Johannes Stallkamp, Marc Schlipsing, Jan Salmen, and Christian Igel. The German Traffic Sign Recognition Benchmark: A multi-class classification competition. In *The 2011 International Joint Conference on Neural Networks*, pages 1453–1460, July 2011. doi: 10.1109/IJCNN.2011.6033395. ISSN: 2161-4407.

Chuanqi Tan, Fuchun Sun, Tao Kong, Wenchang Zhang, Chao Yang, and Chunfang Liu. A survey on deep transfer learning. In *Artificial Neural Networks and Machine Learning—ICANN 2018: 27th International Conference on Artificial Neural Networks, Rhodes, Greece, October 4–7, 2018, Proceedings, Part III* 27, pages 270–279. Springer, 2018.

Bastiaan S. Veeling, Jasper Linmans, Jim Winkens, Taco Cohen, and Max Welling. Rotation Equivariant CNNs for Digital Pathology. In Alejandro F. Frangi, Julia A. Schnabel, Christos Davatzikos, Carlos Alberola-López, and Gabor Fichtinger, editors, *Medical Image Computing and Computer Assisted Intervention – MICCAI 2018*, pages 210–218, Cham, 2018. Springer International Publishing. ISBN 978-3-030-00934-2. doi: 10.1007/978-3-030-00934-2_24.

Ke Wang, Nikolaos Dimitriadis, Guillermo Ortiz-Jimenez, François Fleuret, and Pascal Frossard. Localizing task information for improved model merging and compression. In *Proceedings of the 41st International Conference on Machine Learning*, Proceedings of Machine Learning Research, 2024.

Han Xiao, Kashif Rasul, and Roland Vollgraf. Fashion-MNIST: a Novel Image Dataset for Benchmarking Machine Learning Algorithms, September 2017. URL <http://arxiv.org/abs/1708.07747>. arXiv:1708.07747 [cs, stat].

Jianxiong Xiao, Krista A. Ehinger, James Hays, Antonio Torralba, and Aude Oliva. SUN Database: Exploring a Large Collection of Scene Categories. *International Journal of Computer Vision*, 119(1):3–22, August 2016. ISSN 1573-1405. doi: 10.1007/s11263-014-0748-y. URL <https://doi.org/10.1007/s11263-014-0748-y>.

Prateek Yadav, Derek Tam, Leshem Choshen, Colin A. Raffel, and Mohit Bansal. Ties-merging: Resolving interference when merging models. In *Advances in Neural Information Processing Systems 36: Annual Conference on Neural Information Processing Systems 2023, NeurIPS 2023, New Orleans, LA, USA, December 10 - 16, 2023*, 2023.

Jason Yosinski, Jeff Clune, Yoshua Bengio, and Hod Lipson. How transferable are features in deep neural networks? *Advances in neural information processing systems*, 27, 2014.

Le Yu, Bowen Yu, Haiyang Yu, Fei Huang, and Yongbin Li. Language models are super mario: Absorbing abilities from homologous models as a free lunch. In *Proceedings of the 41st International Conference on Machine Learning*, Proceedings of Machine Learning Research, 2024.

Luca Zhou, Daniele Solombrino, Donato Crisostomi, Maria Sofia Bucarelli, Fabrizio Silvestri, and Emanuele Rodolà. Atm: Improving model merging by alternating tuning and merging, 2024. URL <https://arxiv.org/abs/2411.03055>.

Appendix

We include here additional details on our algorithm, as well as some supplementary results referenced from the main text.

5.1 Results

Benchmark We evaluate on three collections of tasks, containing 8, 14, and 20 tasks respectively. The latter is the most extensive setup considered in Wang et al. [2024], Gargiulo et al. [2025], Daniel et al. [2025]. The 8-task benchmark, introduced in Ilharco et al. [2023], comprises the following datasets: Cars Krause et al. [2013], DTD Cimpoi et al. [2014], EuroSAT Helber et al. [2019], GTSRB Stallkamp et al. [2011], MNIST Lecun et al. [1998], RESISC45 Cheng et al. [2017], SUN397 Xiao et al. [2016], and SVHN Netzer et al. [2011]. Moving to 14 tasks, we add CIFAR100 Krizhevsky and Hinton [2009], STL10 Coates et al. [2011], Flowers102 Nilsback and Zisserman [2008], OxfordIIITPet Parkhi et al. [2012], PCAM Veeling et al. [2018], and FER2013 Goodfellow et al. [2013]. The 20-task suite further includes EMNIST Cohen et al. [2017], CIFAR10 Krizhevsky and Hinton [2009], Food101 Bossard et al. [2014], FashionMNIST Xiao et al. [2017], RenderedSST2 Socher et al. [2013], and KMNIST Klanuwat et al. [2018]. We quantify results using both average absolute accuracy and average normalized accuracy.

Per-layer task accuracy Results are shown in Fig. 3; we refer to the main text for a discussion.

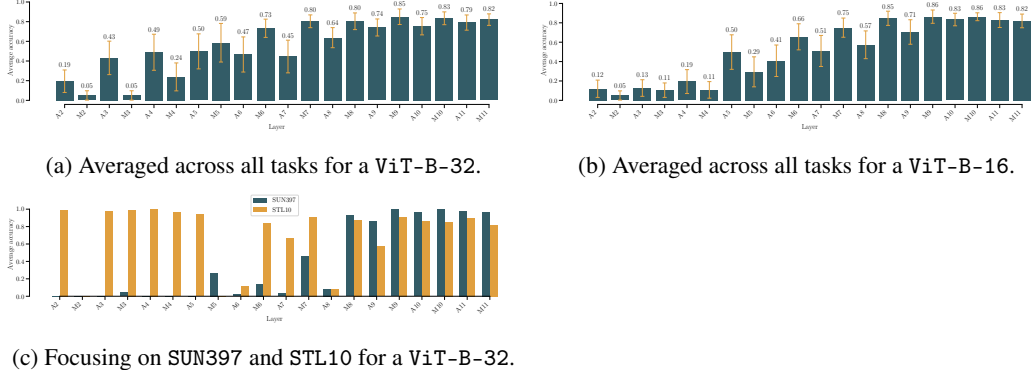


Figure 3: Per-layer task accuracies for ViT-B-32 on the 20-task benchmark. Layers starting with ‘A’ indicate attention layers, while those starting with ‘M’ refer to MLPs.

5.2 Algorithms

The key algorithms implementing our method are reported below; we refer to the main text for a discussion.

Algorithm 1 Fixed Merging Step

Require: Pretrained model weights θ_{pre} , task-specific updates $\{\Delta_i\}_{i=1}^T$, user-specified threshold ε
Ensure: Fixed merged model weights θ_{MT}

- 1: **Accounting for redundant directions**
- 2: $\mathcal{M} = \{\}$
- 3: **for** $i = 1, \dots, T$ **do**
- 4: $\delta_i \leftarrow \text{vec}(\Delta_i)$
- 5: **if** $\max_{\{j \in \mathcal{M}\}} \text{sim}(\delta_i, \delta_j) < \varepsilon$ **then**
- 6: $\mathcal{M} \leftarrow \mathcal{M} \cup \{i\}$
- 7: **end if**
- 8: **end for**
- 9: **Merging step using TSV-M** Gargiulo et al. [2025] **on the** $\{\Delta_i\}_{i \in \mathcal{M}}$
- 10: **for** $i \in \mathcal{M}$ **do**
- 11: $\Delta_i = U_i \Sigma_i V_i^\top$
- 12: $\tilde{U}_i \leftarrow U_i[:, 1:k]$, $\tilde{\Sigma}_i \leftarrow \Sigma_i[1:k, 1:k]$, $\tilde{V}_i \leftarrow V_i[:, 1:k]$
- 13: **end for**
- 14: $U \leftarrow [\tilde{U}_1 | \tilde{U}_2 | \dots | \tilde{U}_T]$
- 15: $\Sigma \leftarrow \text{block_diag}(\tilde{\Sigma}_1, \tilde{\Sigma}_2, \dots, \tilde{\Sigma}_T)$
- 16: $V \leftarrow [\tilde{V}_1 | \tilde{V}_2 | \dots | \tilde{V}_T]$
- 17: $U_\perp \leftarrow \text{orthogonalize}(U)$
- 18: $V_\perp \leftarrow \text{orthogonalize}(V)$
- 19: $\hat{\Delta} \leftarrow U_\perp \Sigma V_\perp^\top$
- 20: $\theta_{\text{MT}} \leftarrow \theta_{\text{pre}} + \alpha \hat{\Delta}$
- 21: **return** θ_{MT}

Algorithm 2 Adaptive Merging Step

Require: Pretrained model weights θ_{pre} , task-specific updates $\{\Delta_i\}_{i=1}^T$, fixed merged model θ_{MT} , top- k parameter k , threshold η , task-specific classification heads $\{h_i\}_{i=1}^T$, sample \mathbf{x}

Ensure: Predicted class c^*

- 1: $\mathbf{z}_\ell \leftarrow \text{ForwardPass}(\theta_{\text{MT}}, \mathbf{x})$ # first pass
- 2: **for** $i = 1, \dots, T$ **do**
- 3: $r_i \leftarrow \|\mathbf{z}_\ell - V_i V_i^\top \mathbf{z}_\ell\|_2$ # residual as Eq. 4
- 4: **end for**
- 5: $w \leftarrow \text{softmax}(-r)$
- 6: $\Omega \leftarrow \{i : w_i \geq \eta\}$ # Select tasks above threshold
- 7: $\Omega \leftarrow \text{TopK}(\Omega, w, k)$ # Keep only top- k weighted tasks
- 8: **Merge selected subspaces**
- 9: $\Delta_{\text{ada}} \leftarrow \sum_{i \in \Omega} U_i \Sigma_i V_i^\top$
- 10: Compute adaptive model: $\theta_{\text{MASS}} \leftarrow \theta_{\text{pre}} + \alpha \Delta_{\text{ada}}$
- 11: **Classification procedure**
- 12: $\mathbf{z}_{L-1} \leftarrow \text{ForwardPass}(\theta_{\text{MASS}}, \mathbf{x})$ # Compute shared representation
- 13: $\mathbf{z}_i \leftarrow h_i(\mathbf{z}_{L-1})$ # Evaluate each head
- 14: $(i^*, c^*) \leftarrow \arg \max_{(i,c) \in \Omega \times \{1, \dots, C_i\}} z_i[c]$ # Highest logit across heads
- 15: **return** c^*
